Colloid Polym Sci 278:301–311 (2000)

ORIGINAL CONTRIBUTION

K. Balashev
N. Panchev
I. Petkov
I. Panaiotov

Photochemical behaviour of polyacryloylacetone and polyethylacrylacetate monolayers at the air–water interface

Received: 11 November 1998
Accepted in revised form: 20 October 1999

K. Balashev · N. Panchev
I. Panaiotov (✉)
Biophysical Chemistry Laboratory
University of Sofia, J. Bourchier 1 str
1126 Sofia, Bulgaria

I. Petkov
Department of Organic Chemistry
University of Sofia, J. Bourchier 1 str
1126 Sofia, Bulgaria

K. Balashev
CISMI, Laboratory for Material Science
Department of Chemistry
University of Copenhagen, Fruebergvej 3
DK-2100 Copenhagen ∅, Denmark

Abstract The surface organization of enol units of polyacryloylacetone (PAA) and polyethylacrylacetate (PEAA) monolayers at the air–water interface is examined using surface pressure, surface potential and rheological measurements and theoretical calculations based on molecular models. The mechanism and kinetics of the photochemical enol–keto tautomerization of PAA and PEAA polymers organized in a monolayer of closely packed monomer units are studied by measuring the surface area increase at constant surface pressure. The results indicate an increase in the area per unit during the consecutive enol-to-keto photoconversion and the slow interfacial reorganization of these forms to a more favourable state.

Key words Polyacryloylacetone · Polyethylacrylacetate · Spread monolayer · Photochemical tautomerization · Kinetics

Introduction

Recently, the photochemical behaviour of polymers containing a β-dicarbonyl group – polyacryloylacetone (PAA) and polyethylacrylacetate (PEAA) – upon UV irradiation has been investigated. The kinetics and mechanism of the photoketonization (Fig. 1) in solution and in thick polymer films obtained after evaporation of organic solvents were studied using classical spectrophotometric methods [1–3].

In principle, the mechanism of a photochemical reaction strongly depends on the organization and molecular orientation. In this sense, the polymer monolayer at the air–water interface is a convenient, simple model for studying the kinetics and mechanism of PAA and PEAA photoketonization in organized molecular media.

This report has two purposes:

1. To analyse the interfacial organization of enol units in PAA and PEAA monolayers using surface pressure–area (π–A) and surface potential–area (ΔV–A) isotherm measurements, a surface rheological approach and theoretical calculations based on molecular models.
2. To study the kinetics and mechanism of photochemical enol–keto tautomerization at the air–water interface at constant surface pressure, assuming that the enol unit requires a smaller surface area than the keto unit and, consequently, during the irradiation of the monolayer, constituted of closely packed enol monomers, an increase in surface area should be expected.

Materials and methods

Polymers and solvents

PAA and PEAA were obtained from the Department of Applied Chemistry, Technical College, University of Tokushima [4]. The molecular weights of PAA and PEAA determined by gel perme-

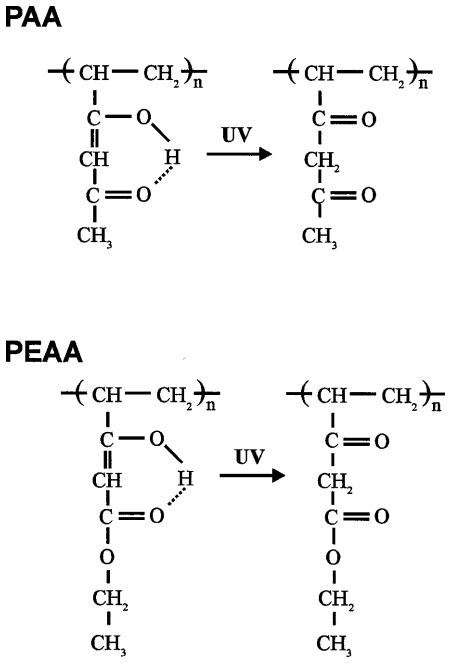

Fig. 1 Photochemical reaction of the enol–keto tautomerization of polyacryloylacetone (*PAA*) and polyacrylethylacetate (*PEAA*)

ation chromatography were more than 100 000. Chromatographically pure chloroform was used as a spreading solvent for PAA and PEAA. The polymers were dissolved in chloroform to give a solution of 0.5 g/l. Double-distilled water was used as a subphase and the subphase temperature was maintained at 20 ± 0.5 °C.

π–A isotherm measurements

PAA and PEAA were spread using an Exmire microsyringe on a double-distilled water subphase (pH ≈ 6) over the entire area available (927 cm^2). In order to avoid any doubts about the accuracy of the results obtained two methods of isotherm measurements were applied. The first one used the Langmuir film balance and the second one was the Wilhelmy method with a platinum plate and a Beckman LM 600 electrobalance connected to a personal computer (PC) provided with specially written software for real-time data measurement. The values of the surface pressure after spreading were less than 0.2 mN/m. Monolayers were left for about 15 min before measurement. π–A isotherms were measured by continuous compression of the spread monolayers at a constant rate, $U_b = 150\,cm^2$/min. In both cases, the isotherms obtained were identical.

ΔV–A isotherm measurements

The surface potential was measured at the air–water interface using a gold-coated ^{241}Am ionizing electrode, a reference electrode and a KP 511 electrometer (Kriona, Bulgaria) connected to a PC provided with specially written software for real-time data acquisition. The compression rate was 150 cm^2/min. The accuracy of the initial surface potential, ΔV_o, measurement was ± 15 mV; however, the accuracy of the surface potential variation rate, $d\Delta V/dt$, was 1 mV/s. As usual, the surface potential of the pure aqueous surface fluctuated for about 30 min. Then it became constant and spreading of the monolayer could be performed.

Rheological measurements

The dynamic response of a polymer monolayer to a dilatational mechanical stress was studied by a theoretical approach based on 2D rheology [5, 6]. We consider the rheological response of the monolayer as a whole, neglecting the surface pressure distribution along the monolayer. To describe the surface pressure change, $\Delta\pi = \pi(t) - \pi_i$, (Fig. 2), during the time, T, of the compression with a constant velocity, U_b, followed by a relaxation, we suppose that, at any moment, $\Delta\pi = \pi(t) - \pi_i$ can be expressed as the sum of one equilibrium, $\Delta\pi_e$, and one nonequilibrium, $\Delta\pi_{ne}$, contribution.

$$\Delta\pi = \Delta\pi_e + \Delta\pi_{ne} \tag{1}$$

The equilibrium part, $\Delta\pi_e$, is related to the equilibrium surface dilatational elasticity, E_e. Thus,

$$\Delta\pi_e = E_e \frac{U_b t}{A_i} \quad , \tag{2}$$

where A_i is initial surface area before the compression and $U_b t/A_i \equiv \Delta A/A_i$ is the corresponding strain (Fig. 2). The upper

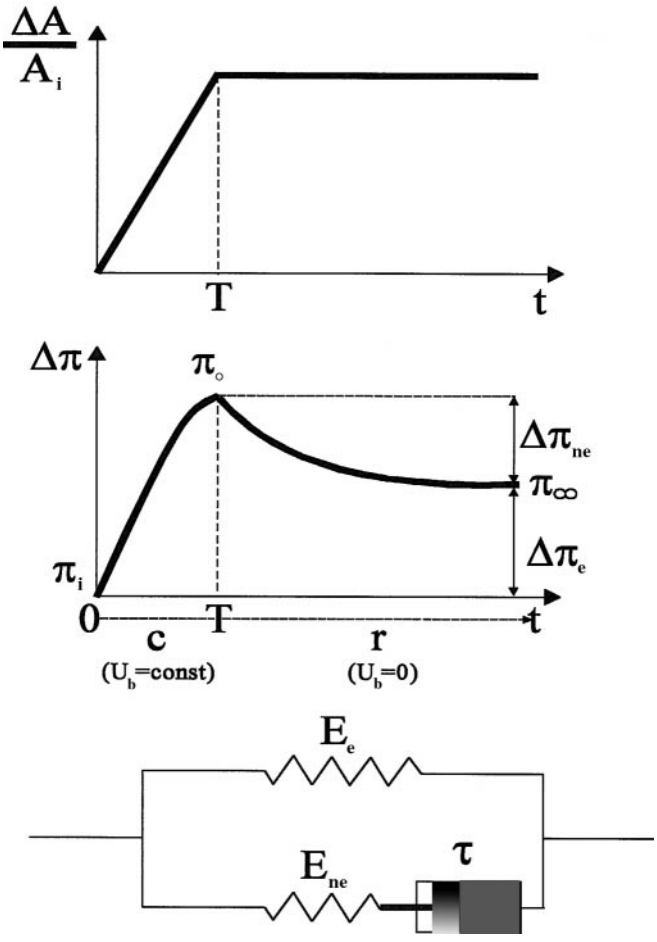

Fig. 2 Rheological model of the monolayer. Deformation ($\Delta A/A_i$) and change in the surface pressure (π) with time (t) during a fast compression (c) with constant velocity (U_b), followed by a relaxation (r). T is the time of compression. For the other notations see the text

branch of the mechanical model in Fig. 2 represents this elastic behaviour.

The nonequilibrium part of the total surface pressure change, $\Delta\pi_{ne}$, is associated with the accumulation of elastic energy during the compression. The dissipation of this accumulated energy through expulsion of segments in the adjacent phase occurs during compression as well as relaxation. This viscoelastic behaviour can be modelled using Maxwell's equation:

$$\frac{d\Delta\pi_{ne}}{dt} + \frac{\Delta\pi}{\tau} = E_{ne}\frac{U_b}{A_i} \quad , \tag{3}$$

where $\Delta\pi_{ne}$ is the applied stress, E_{ne} is the nonequilibrium surface dilatational elasticity and τ is the specific time of relaxation. The lower branch of the mechanical model used (Fig. 2) represents this viscoelastic behaviour. The two branches of the mechanical model are coupled in parallel according to Eq. (1), which corresponds to the addition of stresses.

The general solution of Eqs. (1)–(3) is obtained from Ref. [6]. When T is much smaller than τ (rapid compression or expansion), the following expression for τ during the relaxation process is obtained:

$$\frac{\Delta\pi(t) - \Delta\pi_\infty}{\Delta\pi_0 - \Delta\pi_\infty} \equiv \frac{\pi(t) - \pi_\infty}{\pi_0 - \pi_\infty} = e^{-\frac{t}{\tau}} \quad . \tag{4}$$

If the relaxation process with two relaxation times τ_1 and τ_2 associated with two distinctive molecular mechanisms occurs, Eq. (4) can be extended as follows:

$$\Delta\pi(t) = a + b\exp\left(-\frac{t}{\tau_1}\right) + c\exp\left(-\frac{t}{\tau_2}\right) \quad . \tag{5}$$

Spectrophotometric measurements during the photoketonization of PAA and PEAA solutions

The samples (2 ml PAA) and PEAA solution with $c = 2.5 \times 10^{-3}$ (g/l) were thermostated at $20 \pm 0.5\,^{\circ}C$ in a quartz-glass cuvette and irradiated with monochromatic (254 nm) UV light under standard conditions. The photochemical reaction was carried out on the setup using a medium-pressure mercury lamp as the light source in combination with an IR filter. The UV absorption spectra were measured on a Specord UV–vis spectrophotometer.

π–A measurements of PAA and PEAA monolayers during the photoketonization in solution

The samples (2 ml PAA and PEAA solutions with $c = 0.5$ g/l) were irradiated at 15-min intervals following the previously described procedure. After irradiation, the solutions were spread at the air–water interface and the π–A isotherms were measured.

Measurements of the surface pressure at constant area and of the surface area at constant surface pressure during the photochemical reaction in PAA and PEAA monolayers

PAA and PEAA monolayers were spread on an aqueous subphase in a Teflon rectangular trough (6 cm × 25 cm × 0.7 cm). The monolayers were compressed to a state of maximum packed polymer units at $\pi = 10$ mN/m. Then they were exposed to monochromatic radiation (254 nm) using the same light source. The lamp was fixed above the monolayer at a distance of 10 cm in order for the whole surface area to be irradiated (Fig. 3). The radiation intensity was measured to be 1.29×10^{-16} (quanta $s^{-1}\,cm^{-2}$). The duration of irradiation was in time intervals of 1–5 min. The increase in the surface pressure at constant area and the increase in the area at constant pressure versus time were measured.

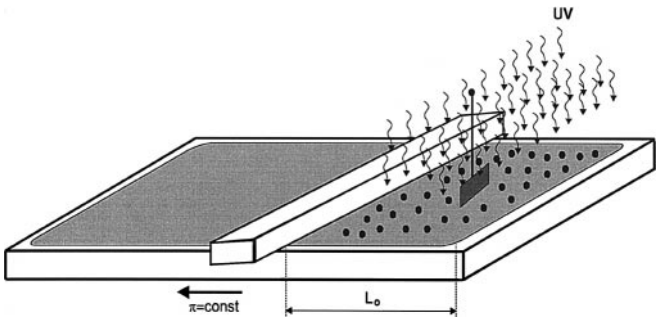

Fig. 3 Schematic representation of the surface balance for measuring the increase in the surface pressure (π) at constant area or the increase in the area at constant surface pressure during the photochemical reaction of the enol–keto tautomerization of PAA and PEAA monolayers spread at the air–water interface. W-Wilhelmy plate, L_0-the length of the monolayer

In all experiments the temperature was controlled in order to avoid any artefacts due to temperature effects. Both the surface pressure and the area increase versus time were related to the kinetics of the interfacial monolayer reorganization induced by photochemical tautomerization.

Molecular models

Molecular modelling was performed using the PCMODEL software (Serena Software). The force field used in PCMODEL is called MMX and is derived from the MM2 (QCPE-395, 1977) force field of N. L. Allinger, with the pi-VESCF routines taken from MMP1 (QCPE-318) also by N. L. Allinger. The program gives the structure of the monomer units. The monomers are situated at the air–water interface, taking into account their hydrophilic–hydrophobic balance.

Results and discussion

Comparative study of the interfacial state of PAA and PEAA monolayers

Surface pressure isotherm measurements

In order to compare the states of PAA and PEAA monolayers before initiating the photochemical reaction by irradiation of the monolayer with UV light the π–A isotherms were measured (Fig. 4).

The inflection point at about 14 $Å^2$/monomer in the isotherm of the PAA monolayer (curve 1) corresponds to closely packed monomers according to the area occupied by one enol acryloylacetone unit. The observed flat plateau at $\pi = 18$–19 mN/m is a 2D–3D phase transition due to the formation in the air-adjacent phase of 3D structures that could be constituted of both expelled portions (loops) and whole polymer molecules. We assume the large number of enol units (96%) in PAA favours their association in 3D structures as a result of hydrogen bonds between neighbouring monomers. Atomic force microscopy imaging confirms this idea

based on the π–A isotherm. Below the plateau no microdomains were observed, but after the plateau the appearance of 3D structures with a typical overheight of 16 Å confirmed the expulsion of polymer segments or whole molecules into the third dimension [7].

The π–A isotherm of the PEAA monolayer is represented by curve 2 in Fig. 4. The inflection point observed at about 15 $Å^2$/monomer corresponds to the area occupied by one ethylacrylacetate unit. The absence of the 2D–3D phase transition and 3D structures can be related to the small number of enol units (30%) in PEAA.

Rheological measurements

Additional information about the state of the PAA and PEAA monolayers at the monolayer closed-packed conformation was obtained by measuring the rheological properties. Some typical results are presented in Fig. 5. Small, fast compression followed by relaxation was produced at $\pi = 10\,\mathrm{mN/m}$. According to the general concepts, the surface pressure measured during the monolayer compression and relaxation can be expressed as a sum of equilibrium, $\Delta\pi_e$, and nonequilibrium, $\Delta\pi_{ne}$, contributions. The equilibrium part of the surface pressure is related to the density of the segments anchored at the interface and their ability to stay in that conformation. The nonequilibrium part can be related to the expulsion of the segments through the interface as a loop shape. From the experimental data in Fig. 5, the nonequilibrium part of the surface pressure, $f_{ne} = (\Delta\pi_{ne}/\Delta\pi)100\%$, is estimated to be 11% in the case of PAA monolayers and 38% for PEAA monolayers. The data show that at the monomer closed-packed conformation of PAA at the air–water interface a higher value of the equilibrium part of the surface pressure, $f_e = 89\%$, is obtained. We assume that a large number of enol units (96%) leads to a higher density of the segments anchored to the interface and stabilized by hydrogen bonds. The data for the PEAA monolayers show that the nonequilibrium contribution increases approximately 4 times. It could be related, one the hand, to the small number of enol units (30%) and, consequently, to the negligible role of the hydrogen bonds or, on the other hand, to the possibility of the reorganization of keto units at the air–water interface through some unknown molecular mechanism. The relaxation times related to the dissipation of the accumulated energy during monolayer compression are calculated using Eqs. (4) and (5). The experimental results (data not shown) are in good agreement with theoretical predictions for one relaxation time in the case of the PAA monolayer and for two relaxation times for the

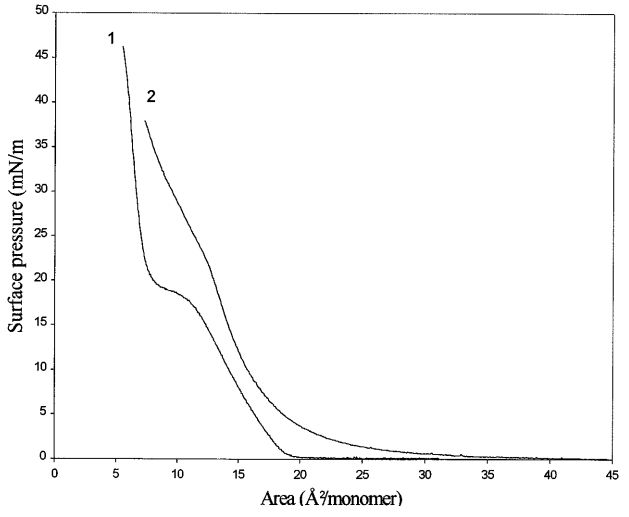

Fig. 4 Surface pressure (π)–area (A) isotherms of the PAA monolayer (*curve 1*) and the PEAA monolayer (*curve 2*)

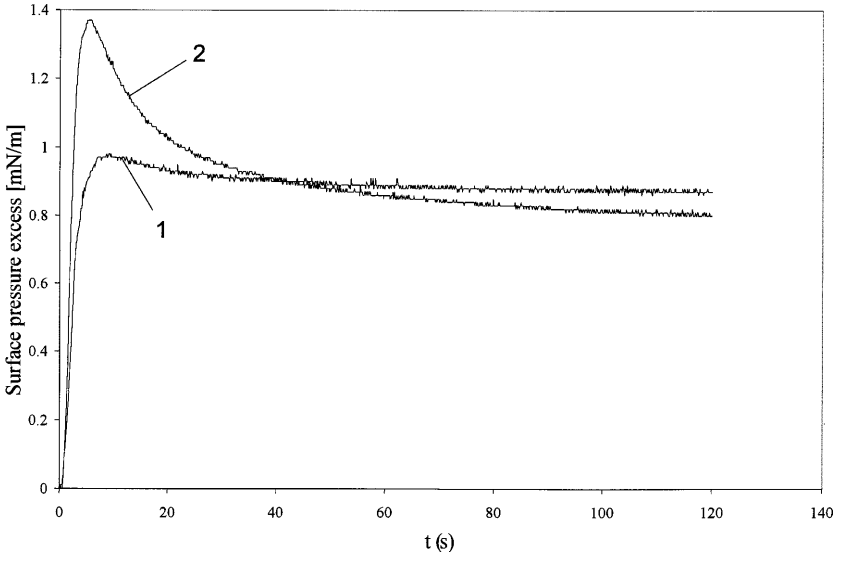

Fig. 5 Surface pressure excess ($\Delta\pi$) as a function of time (t) during a fast compression followed by relaxation of the PAA monolayer (*curve 1*) and the PEAA monolayer (*curve 2*) at $\pi_0 = 10$ mN/m ($U_b = 1.5$ cm/min, $L_0 = 30$ cm)

PEAA monolayer. A relaxation process with one relaxation time ($\tau = 25$ s) is detected for the PAA monolayer at $\pi_0 = 10$ mN/m, while in the case of the PEAA monolayer at the same surface pressure, the theoretical model with two relaxation times ($\tau_1 = 7$ s and $\tau_2 = 44$ s) describes well the data obtained. It should be noted that the molecular mechanisms corresponding to these relaxation times are unknown. We assume that the fast time (7 s) and slow times (25–44 s) are related to the formation of loops and, respectively, to a consecutive reorganization of the monolayer as a whole. In terms of crossing segments through the interface, the faster time means a facilitated expulsion of segments.

Surface potential isotherm measurements and molecular models

The ΔV–A isotherms of the PAA and PEAA monolayers are compared in Fig. 6.

The ΔV–A isotherm of the PAA monolayer (Fig. 6 curve 1) has three branches corresponding to a large surface potential increase (between 27 and 25 Å^2/monomer), a small surface potential increase (between 25 and 14 Å^2/monomer) and saturation (below 14 Å^2/monomer). The surface potential saturation appears at 14 Å^2/monomer, corresponding to the inflection point in the π–A isotherm (Fig. 4).

The surface potential isotherm of PEAA (Fig. 6, curve 2) has only two branches, corresponding to the surface potential increase (between 40 and 15 Å^2/monomer) and the saturation that appears at 15 Å^2/monomer, corresponding to the state of closely packed ethylacrylacetate units.

In Fig. 7 the sum of the vertical components of single-bond dipole moments (μ) in one polymer residue of PAA (curve 1) or PEAA (curve 2) was calculated from surface potential measurements by applying the Helmholtz equation:

$$\Delta V = 4\pi \frac{\mu}{\varepsilon A} \quad , \tag{6}$$

where ε is the dielectric constant and A is the area of one acryloylacetone or one ethylacrylacetate unit. The dielectric constant was taken to be equal to that of a polyethylene chain in the bulk phase ($\varepsilon = 2$) [8, 9].

In principle, the main-chain backbone as well as the shorter side chains of polymer molecules tend to be oriented in a manner so their polar parts interact predominantly with the aqueous phase, whereas the nonpolar ones interact with the nonaqueous phase. Following this concept a possible disposition of the PAA and PEAA polymer molecules at the air–water interface could be proposed. As an example, the interfacial disposition of three PAA residues is shown in Fig. 8A. The main-chain backbone as well as the side chains are situated at the air–water interface and the carbonyl and enol groups are anchored to the aqueous phase. The dipole moment, μ, for PAA can be obtained using the following algebraic sum:

$$\mu_{\mathrm{PAA}} = \mu_{\mathrm{C{=}O}} \cos\theta_1 + \mu_{\mathrm{C{-}O{-}}} \cos\theta_2 + \mu_{\mathrm{{-}O{-}H}} \cos\theta_3 \quad .$$

Using the data for the single-bond dipole moments [10] $\mu_{\mathrm{C{=}O}} = 433$ mD, $\mu_{\mathrm{C{-}O{-}}} = 378$ mD, $\mu_{\mathrm{{-}O{-}H}} = 487$ mD and the values of $\theta_1 \approx \theta_2 = 40°$ and $\theta_3 = 59°$, where θ_1 and θ_2 are the angles between the normal line of the surface and each of the C=O and C–O– groups, respectively (Fig. 8B) and θ_3 is the angle between the normal line of the surface and the –O–H group (Fig. 8C), one can obtain the μ_{PAA} value:

$$\mu_{\mathrm{PAA}} = 433\cos 40° + 378\cos 40° - 487\cos 59° \approx 371 \text{ mD} \quad .$$

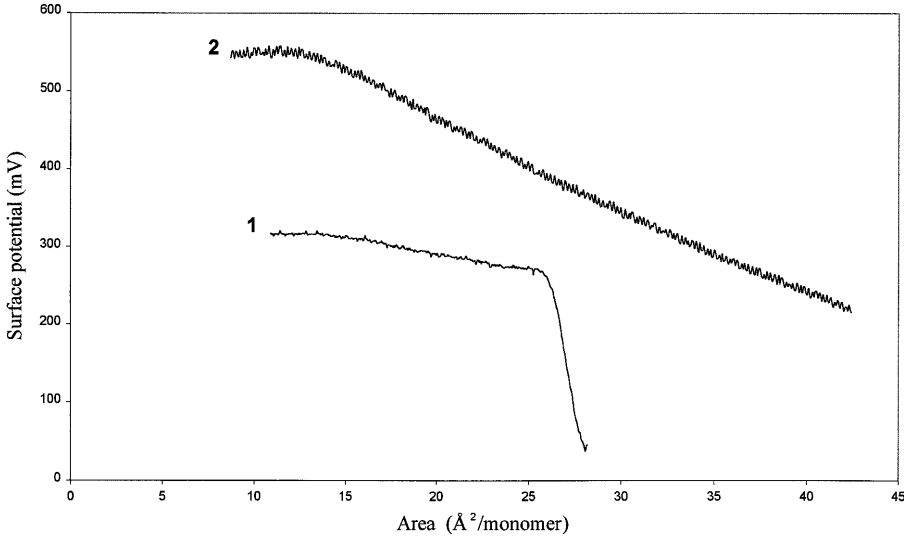

Fig. 6 Surface potential (ΔV)–area (A) isotherms for the PAA monolayer (*curve 1*) and for the PEAA monolayer (*curve 2*)

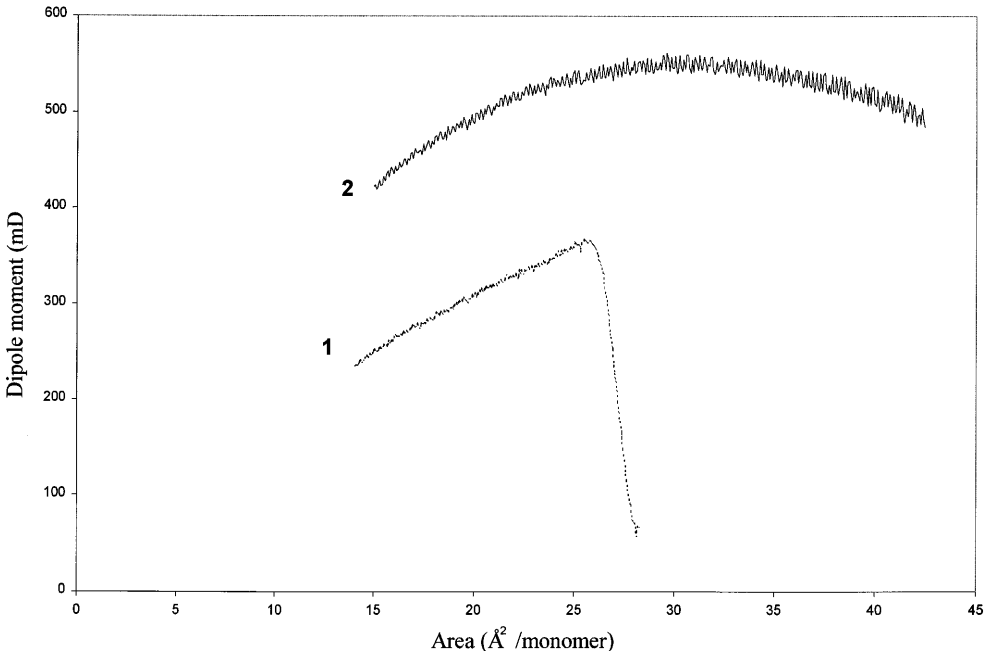

Fig. 7 Sum of the vertical components of the dipole moments of the bonds (μ) versus (A) calculated from the data in Fig. 6 and using Eq. (6) for the PAA (*curve 1*) and PEAA (*curve 2*) monolayers

The large increase in the surface potential from 50 to 265 mV between the areas of 27 and 25 Å^2/monomer corresponds to an increase in μ from 60 to 362 mD. The maximum value of μ is 362 mD, which is in good agreement with the theoretically obtained value of 371 mD. This situation corresponds to the monolayer state when the main-chain backbone as well as the shorter side chains are situated at the air–water interface. The further compression of the monolayer from 25 to 14 Å^2/monomer leads to a slower surface potential increase and to a dipole moment decrease. The surface potential reaches a saturation value of 310 mV with a corresponding dipole moment of 220 mD. We assumed that during the monolayer compression below values of 25 Å^2/monomer the CH_3 terminal group of the shorter side polymer chain starts to reduce in the aqueous phase; therefore, the dipole moment decrease is due to another angle, φ, between the normal line of the surface and the carbonyl group (Fig. 9A). Substituting the experimental value of the dipole moment of 220 mD, one can estimate φ:

$$220 = 433\cos\varphi + 378\cos 40^\circ - 487\cos 59^\circ$$
$$\varphi \approx 65^\circ \ .$$

A similar calculation for the dipole moment of the PEAA monolayer can be performed. As the keto units predominate (70%) this should be taken into account:

$$\mu_{\mathrm{PEAA}} = 0.3\mu_{\mathrm{PEAA(enol)}} + 0.7\mu_{\mathrm{PEAA(keto)}} \ ,$$

where

$$\mu_{\mathrm{PEAA(enol)}} = \mu_{\mathrm{C{=}O}}\cos\theta_1 + \mu_{\mathrm{C{-}O{-}}}\cos\theta_2 - \mu_{\mathrm{{-}O{-}H}}\cos\theta_3 - \mu_{\mathrm{{-}O{-}CH_2{-}CH_3}}\cos\theta_4$$

$$\mu_{\mathrm{PEAA(keto)}} = \mu_{\mathrm{C{=}O}}\cos\theta_5 + \mu_{\mathrm{C{=}O}}\cos\theta_6 - \mu_{\mathrm{{-}O{-}CH_2{-}CH_3}}\cos\theta_7 \ .$$

Using the data for the single-bond dipole moments ($\mu_{\mathrm{C{=}O}} = 433$, $\mu_{\mathrm{C{-}O{-}}} = 378$, $\mu_{\mathrm{{-}O{-}H}} = 487$ [10] and $\mu_{\mathrm{{-}O{-}CH_2{-}CH_3}} = 170$ mD [9]) and the values of $\theta_1 \approx 15^\circ$, $\theta_2 \approx 0^\circ$, $\theta_3 = 59^\circ$ and $\theta_4 = 72^\circ$ (Fig. 10A), $\theta_5 = 46^\circ$, $\theta_6 = 48^\circ$ and $\theta_7 = 73^\circ$ (Fig. 10B), where θ_1 and θ_2 are the angles between the normal line of the surface and the C═O and C—O— groups, respectively, θ_3 is the angle between the normal line of the surface and the —O—H group, θ_5 and θ_6 are the angles between the normal line of the surface and each of the C═O groups, and θ_4 and θ_7 are the angles between the normal line of the surface and the —O—CH_2—CH_3 groups in one PAA and one PEAA unit, respectively, one can obtain for $\mu_{\mathrm{PEAA(enol)}}$ and $\mu_{\mathrm{PEAA(keto)}}$ the values

$$\mu_{\mathrm{PEAA(keto)}} = 433\cos 46^\circ + 433\cos 48^\circ - 170\cos 73^\circ \approx 541\ \mathrm{mD}$$

$$\mu_{\mathrm{PEAA(enol)}} = 433\cos 15^\circ + 378\cos 0^\circ - 487\cos 59^\circ - 170\cos 72^\circ \approx 497\ \mathrm{mD}$$

and finally

$$\mu_{\mathrm{PEAA}} = 0.3 \times 497 + 0.7 \times 541 = 528\ \mathrm{mD} \ .$$

The surface potential increase from 230 mV to the saturation value of 550 mV between the areas of 40 and 30 Å^2/monomer corresponds to a dipole moment increase from 515 mD to a maximum value of 550 mD, which is in a good agreement with the theoretically obtained value of 528 mD. This situation corresponds to

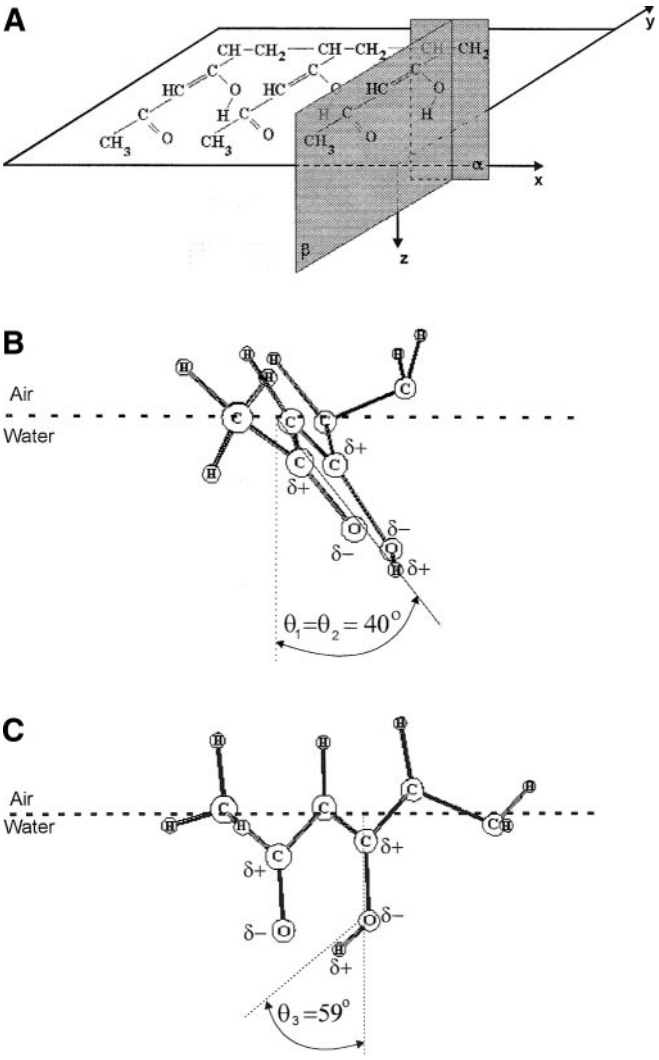

Fig. 8A–C Possible dispositon of a part of a PAA polymer molecule at the air–water interface. α and β are two plane sections perpendicular to the plane of the interface. Both the main-chain backbone, lying in the α plane, and the shorter side chain, lying in the β plane, are oriented at the surface in such a way that the enol and carbonyl groups are anchored to the water phase. **A** Perspective drawing of a part of the PAA polymer molecule with three polymer residues. **B** View along the *y*-direction towards the α plane. **C** View along the *x*-direction towards the β plane. The state corresponds to the maximum value of μ of 362 mD (see text)

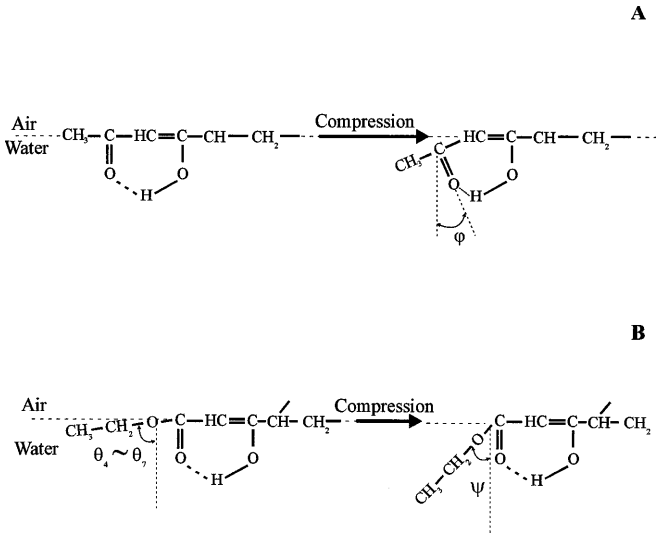

Fig. 9 Schematic view of the dipping of **A** a terminal CH_3 group of the shorter chain during compression of the monolayer of PAA after the values of the area 25° Å^2/monomer and **B** a terminal O—CH_2—CH_3 group of the shorter chain during compression of the monolayer of PEAA after the values of the area of 30 Å^2/monomer

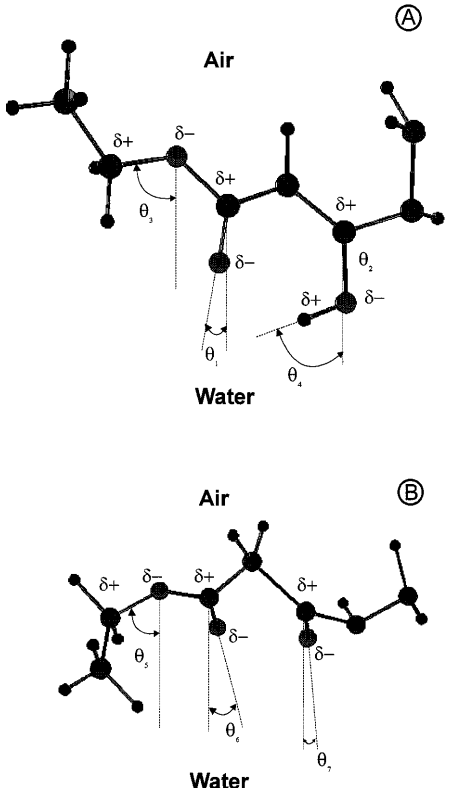

Fig. 10A, B Molecular models of PEAA monolayers. View of enol and keto units situated at the air–water interface

the monolayer state when the main-chain backbone as well as the shorter side chains are situated at the air–water interface. A further monolayer compression from 30 to 15 Å^2/monomer leads to a dipole moment decrease to the value of 425 mD. In a similar way (Fig. 9B) we assumed that during the monolayer compression below the values of 30 Å^2/monomer, the —O—CH_2—CH_3 terminal group of the shorter side polymer chain starts to reduce in the aqueous phase. Then, taking into account that the angles θ_4 and θ_7 are approximately equal, the new angle, ψ, which corresponds to the diping of —O—CH_2—CH_3 group, can be estimated using the experimental value of the dipole moment of 425 mD.

$$425 = (497 + 170\cos 72^\circ - 170\cos\psi) \times 0.3 + (541 + 170\cos 73^\circ - 170\cos\psi) \times 0.7 \approx 27^\circ$$

Kinetics of the photochemical tautomerization of the PAA and PEAA monolayers

The complete kinetics scheme of the photochemical reaction is analysed in an organic solvent bulk solution [3] and a polymer film [1].

$$E_{cis} \xrightarrow{h\nu} E^*_{cis} \rightleftarrows E_{trans} \longrightarrow K \ ,$$

where E_{cis}, E^*_{cis} and E_{trans} are the different energetic and isomeric states of the enol form and K is the keto form.

The transformations between the E_{cis}, E^*_{cis} and E_{trans} forms are very fast in comparison with the experimental characteristic time of the order of 5 min. Therefore, the conversion between the above forms cannot be detected by the measured interfacial parameter (the change in the surface area) and, consequently, E_{cis}, E^*_{cis} and E_{trans} are indistinguishable.

On the other hand, the thermal re-enolization, $K \rightarrow E_{cis}$, is slower in comparison to the ketonization, $E \rightarrow K$, and can be neglected in the kinetics scheme. In fact, the characteristic lifetime of the dicarbonyl keto form is of the order of magnitude of 1 hour in a dilute organic solvent bulk solution [3] and several hours in polymer films [1]. It should be mentioned as well that in the case of a spread monolayer, the polar substrate favours the formation of and, additionally, stabilizes the dicarbonyl keto unit.

In order to adapt the kinetics scheme for the PAA and PEAA monolayers spread at the air–water interface, two subsequent stages are considered. The first one is the photochemical transformation of the enol to the keto form and the second one is a reorganization of the keto form to a more favourable state (K_i) at the interface:

$$E \xrightarrow{k_1} K \underset{k_3}{\overset{k_2}{\rightleftarrows}} K_i \ .$$

The corresponding kinetics equations are

$$\frac{d\Gamma_K}{dt} = k_1\Gamma_E - k_2\Gamma_K + k_3\Gamma_{K_i}$$

$$\frac{d\Gamma_E}{dt} = -k_1\Gamma_E \ ,$$

where Γ_E, Γ_K and Γ_{K_i} are the surface concentrations, expressed as monomer per unit area of the forms E, K and K_i, respectively; k_1, k_2, k_3 are the corresponding rate constants.

Two useful approximations may be developed by the supposition that the photochemical conversion ($E \rightarrow K$) is faster than the interfacial reorganization of the reaction product ($K \leftrightarrow K_i$).

1. During the irradiation time, τ_{irr}, we neglect the reorganization process:

$$E \xrightarrow{k_1} K \ .$$

The corresponding kinetics and mass-balance equations are

$$\frac{d\Gamma_E}{dt} = -k_1\Gamma_E$$

$$\Gamma^0 = \Gamma^0_E + \Gamma^0_K \ , \tag{7}$$

where Γ^0_E and Γ^0_K are the initial surface concentrations of the enol and keto units, respectively. Then,

$$\Gamma_E(t) = \Gamma^0_E e^{-k_1 t} \tag{8}$$

$$\Gamma_K(t) = \Gamma^0_K + \Gamma^0_E(1 - e^{-k_1 t}) \ . \tag{9}$$

2. After irradiation only the reorganization process is taken into account:

$$K \underset{k_3}{\overset{k_2}{\rightleftarrows}} K_i \ .$$

The corresponding kinetics and mass-balance equations are

$$\frac{d\Gamma_K}{dt} = -k_2\Gamma_K + k_3\Gamma_{K_i}$$

$$\Gamma^{irr} = \Gamma_K + \Gamma_{K_i} \ , \tag{10}$$

where Γ^{irr} is the surface concentration of the keto units obtained at the end of the irradiation. Then,

$$\Gamma_K(t) = \Gamma^{irr}\left(\frac{k_3}{k_2 + k_3} + \frac{k_2}{k_2 + k_3}\exp\left[-(k_2 + k_3)t\right]\right) \tag{11}$$

$$\Gamma_{K_i}(t) = \Gamma^{irr}\frac{k_2}{k_2 + k_3}\left(1 - \exp\left[-(k_2 + k_3)t\right]\right) \ . \tag{12}$$

For the first stage ($E \rightarrow K$) we could not determine the kinetics constant, k_1, from direct spectrophotometric experiment at the interface, but we could estimate it from the surface pressure measurements. The photochemical reaction is initiated in a closely packed monolayer, where all polymer residues have identical interfacial orientation and they are uniformly exposed to the radiation.

The experimental data of the surface pressure increase at constant area, and the area increase at constant surface pressure, during and after irradiation (with irradiation times $\tau_{irr} = 1, 3$ and 5 min) are presented in Fig. 11. The kinetics of the interfacial photochemical reaction of the two polymers is different. After the end of the irradiation of the PAA monolayer the surface pressure increases exponentially, whereas in the case of the PEAA monolayer it remains constant. It could be

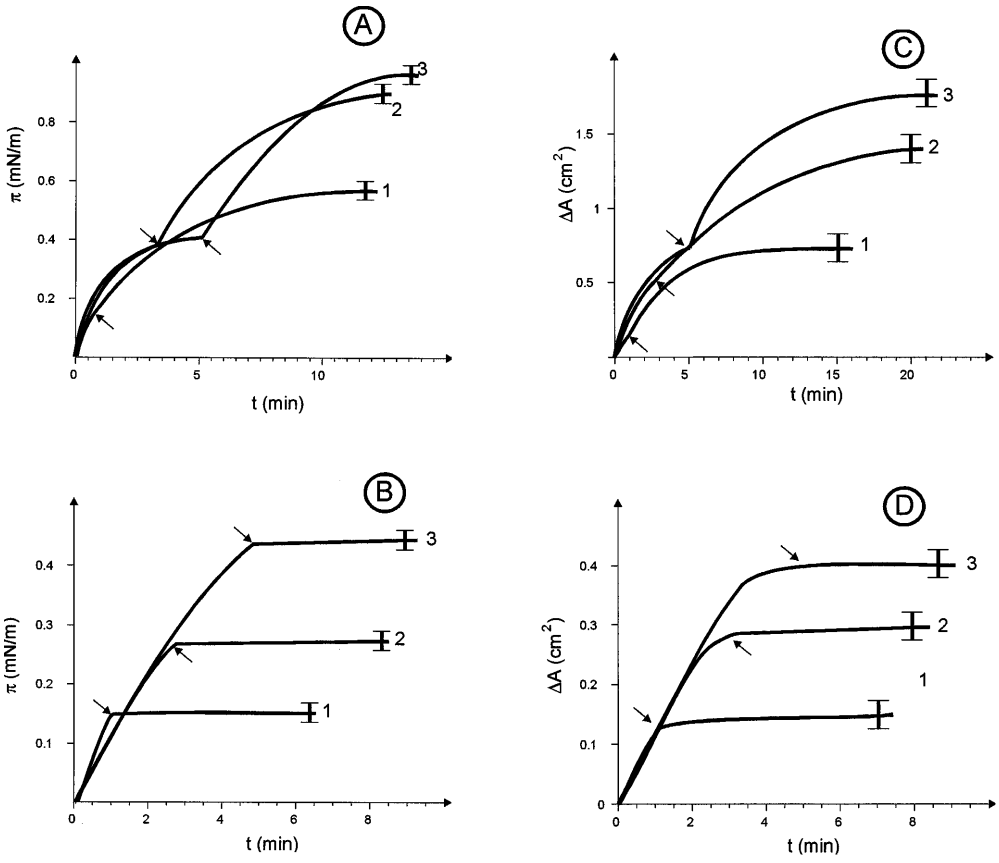

Fig. 11 Increase in the surface pressure ($\Delta\pi$) versus time (t) at constant area (A) for **A** PAA and **B** PEAA and increase in the surface area (ΔA) versus t at constant surface pressure $\pi = 10.0\,\mathrm{mN/m}$ for **C** PAA and **D** PEAA during and after the irradiation of the monolayer spread at the air–water interface. The start of the irradiation is at $t = 0$. The *arrows* show the end of the irradiation at $\tau_{irr} : \tau_{irr} = 1\,\mathrm{min}$ (*curve 1*), 3 min (*curve 2*), 5 min (*curve 3*). The *bars* correspond to the maximum deviation of the experimental data. The initial area is $30\,\mathrm{cm}^2$

assumed that the surface pressure increase is due to a lateral force resulting from the keto form requiring a larger area on the interface in comparison with the enol form. At the irradiated end of the PAA monolayer the observed surface pressure increase is related to the reorganization of keto forms produced from the photochemical reaction. In the case of the PEAA monolayer, the keto forms predominate (70%) before irradiation and their interfacial organization cannot be modified by the small additional production of keto forms during the photochemical process.

In principle, the observed area increase is related to the increase in the area per monomer unit during the consecutive conversion of E into K and K into K_i. Thus, for the first stage of photoconversion (E → K) one can write

$$\frac{\Delta A}{A_0} = a_{\mathrm{K}}(\Gamma_{\mathrm{K}} - \Gamma^0_{\mathrm{K}}) - a_{\mathrm{E}}(\Gamma_{\mathrm{K}} - \Gamma^0_{\mathrm{K}}) \ ,$$

where a_{E} and a_{K} are surface areas per unit of the enol and keto forms, respectively; ΔA is the increase in the area; A_0 is the initial area of the monolayer.

By using Eq. (9) one can obtain

$$\frac{\Delta A}{A_0} = \Gamma^0_{\mathrm{E}}(a_{\mathrm{K}} - a_{\mathrm{E}})\left(1 - \mathrm{e}^{-k_1 t}\right) \ . \qquad (13)$$

Equation (11) fits the experimental $\Delta A(t)/A$ data for the PAA monolayer obtained with irradiation times of 1 min with $k_1 = 0.84\,\mathrm{min}^{-1}$, 3 min with $k_1 = 0.70\,\mathrm{min}^{-1}$ and 5 min with $k_1 = 0.50\,\mathrm{min}^{-1}$ (data not shown). The value of $k_1 = 0.84\,\mathrm{min}^{-1}$ obtained at a sufficiently short time ($\tau_{irr} = 1\,\mathrm{min}$) of irradiation corresponds better to approximation 1. From the experimental $\Delta A(t)/A_0$ data for the PEAA monolayer a value of $k_1 = 0.25\,\mathrm{min}^{-1}$ is obtained. We also determined k_1 from spectrophotometric measurements in the bulk phase of PAA and PEAA chloroform solutions in order to compare the E → K process in the case where occurs at the interface to the same one occurring in bulk solution. As an illustration the adsorption spectra of PAA is presented in Fig. 12. It shows an intense band in the 270–276 nm region. According to Ref. [3], the high-intensity band at 274 nm is associated with the n-π^* transition in the C—O—conjugated ethylene system (enol form). The UV irradiation of PAA in chloroform solution at 254 nm resulted in adsorption spectra changes which are due to enol–keto conversion. The extinction coefficient of the keto form is very small and therefore only alterations in the concentration of the enol form could be followed spectrophotometrically.

From the experimental data, by applying kinetic model (1) to the E → K conversion in the bulk phase,

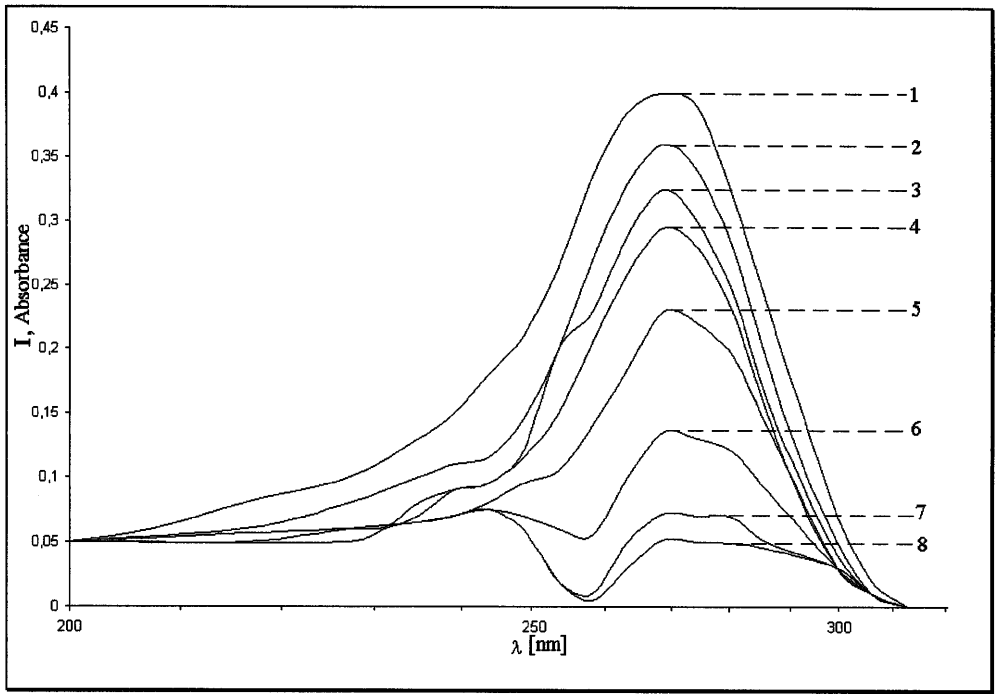

Fig. 12 UV spectra of PAA in $CHCl_3$ ($c = 2.5 \times 10^{-3}$ g/l) measured at different irradiation times, τ_{irr}: nonirradiated (*1*); 0.2 min (*2*); 0.5 min (*3*); 0.8 min (*4*); 1.8 min (*5*); 3.8 min (*6*); 5.8 min (*7*); 7.8 min (*8*)

the reaction rate constant was determined to be $k_1 = 0.28\,\text{min}^{-1}$ [11]. A value of $0.55\,\text{min}^{-1}$ for k_1 was obtained in the case of a chloroform PEAA solution [3]. A comparison of the rate constants of the photoinduced PAA E $\rightarrow$ K tautomerization occurring at the interface ($k_1 = 0.84\,\text{min}^{-1}$) and in the bulk solution ($k_1 = 0.28\,\text{min}^{-1}$) shows that the process is faster if it occurs at the interface. In contrast, the photoinduced PEAA E $\rightarrow$ K tautomerization runs slower at the interface than in the bulk solution. In order to relate the photoconversion occurring in the bulk solution to the interfacial properties, the π–A isotherms of the PAA and PEAA monolayers were measured after spreading the nonirradiated PAA and PEAA solutions as well as the same solution but preliminarily irradiated for 15, 30 and 60 min. The results for the PAA and PEAA monolayers are shown in Fig. 13. The flat plateau observed in the isotherm of the nonirradiated PAA monolayer is a 2D $\rightarrow$ 3D phase transition, which is most likely a result of the hydrogen bonds between the enol units (their amount is 96% initially). This phase transition disappears progressively after 15 and 30 min irradiation. A continuous 60-min irradiation leads to the occurrence of photolytic processes of the keto form, and especially for PEAA a stable monolayer of the photoproducts cannot be formed.

The second stage reorganization of the keto form (K $\leftrightarrow$ K_i) is observed only with the PAA monolayer. In the framework of approximation 2

$$\frac{\Delta A}{A_0} = a_{K_i}\Gamma_{K_i} - a_K\Gamma_K \quad , \tag{14}$$

where a_K and a_{K_i} are the surface areas per unit of the keto and the reorganized keto forms, respectively. After substitution of Eq. (12) in Eq. (14), we obtain

$$\frac{\Delta A}{A_0} = \Gamma^{irr}\frac{k_2}{k_2 + k_3}(a_{K_i} - a_K)\left\{1 - \exp^{[-(k_2+k_3)t]}\right\} \quad . \tag{15}$$

From the experimental data fit after using Eq. (15) we can determine $k_2 + k_3 = 0.32\,\text{min}^{-1}$ (data not shown). The increase in the areas during the consecutive conversion of E, K and K_i can be estimated from the experimental results in Fig. 11B and D and from Eqs. (13) and (15) for a short irradiation time (1 min). For the initial concentrations of the enol forms before irradiation for both PAA and PEAA monolayers we obtain

$$\Gamma_E^0 = 0.96\frac{1}{14}10^{16} = 6.68 \times 10^{16}\ \text{monomers/cm}^2$$

and

$$\Gamma_E^0 = 0.30\frac{1}{14}10^{16} = 2.14 \times 10^{16}\ \text{monomers/cm}^2 \quad ,$$

respectively.

From the experimental data for A_0, ΔA_{irr} and k_1 at $\tau_{irr} = 1\,\text{min}$ and applying Eq. (13), the increases ($a_K - a_E$) in the area resulting from the photoconversion of one enol to one keto unit for both PAA and PEAA monolayers are 0.25 and 0.40 Å^2, respectively.

In order to estimate the area increase ($a_{K_i} - a_K$) resulting from the reorganization of the keto units for the PAA monolayer Eq. (15) can be simplified. At the end of the process ($t \rightarrow \infty$) Eq. (15) reads

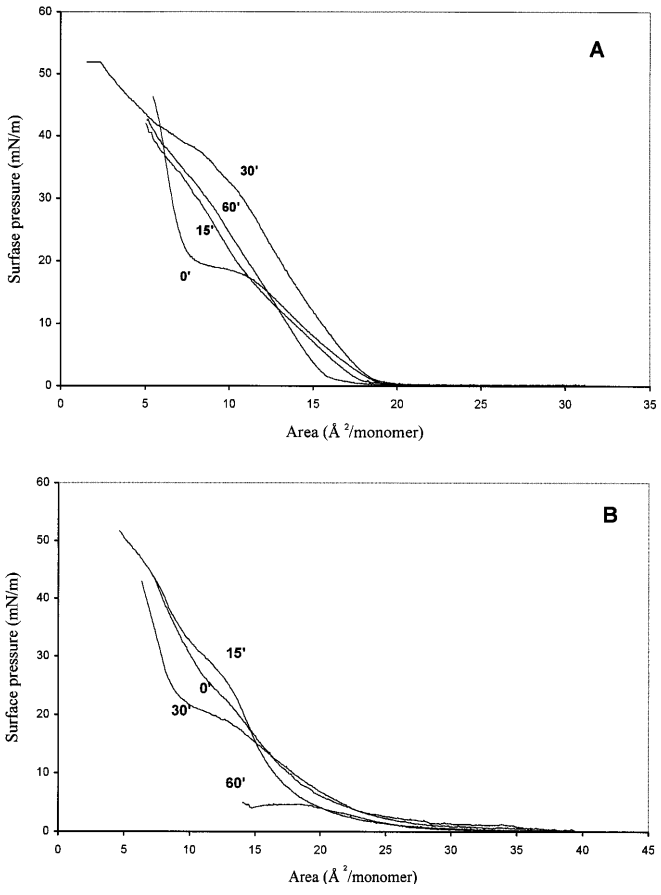

Fig. 13 Surface pressure (π)–area per monomer unit (A) obtained after spreading solutions of **A** PAA and **B** PEAA ($c = 0.5\,\mathrm{g/l}$) without irradiation ($\tau_{\mathrm{irr}} = 0\,\mathrm{min}$) and irradiated for different durations ($\tau_{\mathrm{irr}} = 15, 30$ and 60 min)

$$\frac{\Delta A_\infty}{A_0} = (a_{\mathrm{K}_i} - a_{\mathrm{K}})\frac{k_2}{k_2 + k_3}\Gamma^{\mathrm{irr}} \quad . \tag{16}$$

With the evident relationships $0 < \frac{k_2}{k_2+k_3} < 1$ and $k_2 + k_3 = 0.32\ \mathrm{min}^{-1}$

$$0 < k_2 < 0.32 \tag{17}$$

Eq. (16) becomes

$$\frac{\Delta A_\infty}{A_0} > (a_{\mathrm{K}_i} - a_{\mathrm{K}})\Gamma^{\mathrm{irr}} \quad . \tag{18}$$

After the substitution in Eq. (18) of ΔA_∞, A_0 and Γ^{irr} from Fig. 11B (curve 1) we obtained a reasonable estimation of the area increase per unit resulting from the interfacial reorganization of the keto form:

$$a_{\mathrm{K}_i} - a_{\mathrm{K}} < 1.10\,\mathrm{Å}^2 \quad .$$

Summary

In conclusion, a simple model of closely packed PAA and PEAA monolayers with uniformly orientated enol and keto units which were exposed to UV radiation is used as a tool for the investigation of the mechanism and kinetics of the photochemical enol–keto tautomerization at the interface.

From the experimental area change versus time curves and a developed kinetics approach the area increase per unit and the rate constants of the reaction of PAA and PEAA polymers organized in a monolayer were determined.

Acknowledgement This work was partly supported by the Bulgarian National Foundation for Scientific Research Projects.

References

1. Masuda S, Sertova N, Petkov I (1997) J Polym Sci Part A Polym Chem 35:3683
2. Petkov I, Masuda S, Sertova N, Grigorov L (1995) J Photochem Photobiol A 85:191
3. Petkov I, Masuda S, Sertova N, Grigorov L (1996) J Photochem Photobiol A 95:189
4. Masuda S, Tanaka M, Ota T (1989) J Polym Sci Part A Polym Chem 27:855
5. Balashev K, Bois A, Proust JE, Ivanova Tz, Petkov I, Masuda S, Panaiotov I (1997) Langmuir 13:5362
6. Boury F, Ivanova Tz, Panaiotov I, Proust J, Bois A, Richou J (1995) J Colloid Interface Sci 169:380
7. Balashev K, Panaiotov I, Petkov I, Proust JE, Masuda S (1997) J Dispersion Sci Technol 18:6–7:661
8. Lide DR (ed) Handbook of chemistry and physics, 77th edn. CRC, Boca Raton
9. Davies JT, Rideal E (1961) Interfacial phenomena. Academic, New York
10. Markov P (1982) Thesis. University of Sofia
11. Balashev K, Petkov I, Panaiotov I (1998) Colloid Polym Sci 276:984